The Plant Journal (2003) **36**, 229–239 doi: 10.1046/j.1365-313X.2003.01871.x

Vacuolar cation/H^+ exchange, ion homeostasis, and leaf development are altered in a T-DNA insertional mutant of *AtNHX1*, the *Arabidopsis* vacuolar Na^+/H^+ antiporter

Maris P. Apse, Jordan B. Sottosanto and Eduardo Blumwald*
Department of Pomology, University of California, One Shields Ave, Davis, CA 95616, USA

Received 14 May 2003; revised 22 July 2003; accepted 25 July 2003.
*For correspondence (fax +1 530 752 8502; e-mail eblumwald@ucdavis.edu).

Summary

The function of vacuolar Na^+/H^+ antiporter(s) in plants has been studied primarily in the context of salinity tolerance. By facilitating the accumulation of Na^+ away from the cytosol, plant cells can avert ion toxicity and also utilize vacuolar Na^+ as osmoticum to maintain turgor. As many genes encoding these antiporters have been cloned from salt-sensitive plants, it is likely that they function in some capacity other than salinity tolerance. The wide expression pattern of *Arabidopsis thaliana* sodium proton exchanger 1 (*AtNHX1*) in this study supports this hypothesis. Here, we report the isolation of a T-DNA insertional mutant of *AtNHX1*, a vacuolar Na^+/H^+ antiporter in *Arabidopsis*. Vacuoles isolated from leaves of the *nhx1* plants had a much lower Na^+/H^+ and K^+/H^+ exchange activity. *nhx1* plants also showed an altered leaf development, with reduction in the frequency of large epidermal cells and a reduction in overall leaf area compared to wild-type plants. The overexpression of AtNHX1 in the *nhx1* background complemented these phenotypes. In the presence of NaCl, *nhx1* seedling establishment was impaired. These results place AtNHX1 as the dominant K^+ and Na^+/H^+ antiporter in leaf vacuoles in *Arabidopsis* and also suggest that its contribution to ion homeostasis is important for not only salinity tolerance but development as well.

Keywords: Na^+/H^+ antiporter, vacuole, ion homeostasis, AtNHX1, leaf development.

Introduction

Typically, plant cells maintain a low cytosolic Na^+ concentration. The low cytosolic Na^+ concentration is attained by the operation of Na^+/H^+ antiporters located at both the plasma membrane (Shi *et al.*, 2000) and the tonoplast (Apse *et al.*, 1999). Electrochemical H^+ gradients generated by H^+ pumps at the plasma membrane (H^+-ATPase) and the tonoplast (H^+-ATPase, H^+-PP_iase) provide the energy used by the plasma membrane- and tonoplast-bound Na^+/H^+ antiporters to couple the passive movement of H^+ to the active movement of Na^+ out of the cell and into the vacuole, respectively. Plant vacuolar Na^+/H^+ antiporter activity was first measured in tonoplast-enriched membranes isolated from red beet storage tissue (Blumwald and Poole, 1985). Similar Na^+/H^+ exchange has subsequently been measured in many plants (Blumwald *et al.*, 2000; references therein). The cloning of AtNHX1 (Apse *et al.*, 1999; Gaxiola *et al.*, 1999) followed by its functional complementation of yeast *Δnhx1* mutants (Gaxiola *et al.*, 1999) and the measurement of its Na^+/H^+ exchange activity in vacuoles isolated from transgenic *Arabidopsis* overexpressing AtNHX1 (Apse *et al.*, 1999) and in vacuolar vesicle membranes isolated from yeast expressing AtNHX1 (Darley *et al.*, 2000) clearly confirmed the function of AtNHX1 as an Na^+/H^+ antiporter. Much interest in the occurrence and activity of Na^+/H^+ antiporter activity in plants has been related to the study of salinity tolerance. Increased expression of *AtNHX1* by transformation with *AtNHX1* driven by a strong constitutive promoter has been shown to improve the tolerance to salinity of *Arabidopsis* (Apse *et al.*, 1999), *Brassica* (Zhang *et al.*, 2001), and tomato (Zhang and Blumwald, 2001). Cumulatively, these results suggest that an increased capacity for vacuolar Na^+ sequestration is important for salinity tolerance. This increased capacity is exhibited by salt-tolerant species, for example, *Beta*, *Atriplex gmelini*, and *Mesembryanthemum*, which show strong induction of both Na^+/H^+ antiporter expression and activity in response to NaCl treatment (Barkla *et al.*, 1995; Chauhan *et al.*, 2000; Hamada *et al.*, 2001, Xia *et al.*, 2002).

AtNHX1 was shown to mediate the transport of K^+ as well as Na^+ in tonoplast vesicles isolated from tomato plants that had been transformed with an overexpression construct of AtNHX1 (Zhang and Blumwald, 2001). The capacity of AtNHX1 to mediate both K^+/H^+ and Na^+/H^+ transport was also demonstrated in liposomes reconstituted with purified AtNHX1 (Venema *et al.*, 2002). These results supported the role of AtNHX1 in cellular ion homeostasis, that is, the maintenance of ion concentrations that are optimal for growth and development in all plants, both salt-tolerant and salt-sensitive.

Here, we used a T-DNA insertional mutant of AtNHX1 to assess the role of AtNHX1 in *Arabidopsis*. Measurements of vacuolar cation/H^+ antiporter activity in vacuoles isolated from wild-type and *nhx1* plants together with the growth responses of these plants in the presence and absence of salt stress support the role of AtNHX1 in ion homeostasis.

Results

T-DNA-tagged nhx1 *mutant isolation*

In order to determine the role of AtNHX1 in wild-type plants, we sought to isolate null mutants from the T-DNA tagged lines available at the *Arabidopsis* Knockout Facility (Madison, WI, USA). Using gene-specific primers near the borders of the 5′ and 3′ ends of the coding sequence for *AtNHX1*, we were able to isolate a line with a T-DNA insertion sufficiently proximal to the gene to anticipate an appreciable effect on *AtNHX1* expression. The position of this T-DNA insertion is shown in Figure 1. Sequencing from the left-border primer of the T-DNA insertion confirmed that the T-DNA insertion was located in the 9th exon of the *AtNHX1* gene. Using PCR, we also confirmed that the DNA upstream and downstream of the insertion was intact in the line containing the insertion (data not shown). Kanamycin resistance segregated with the insertion (tested with the same PCR reaction as that in the screening process). To confirm that lines whose progeny were homozygous for kanamycin resistance were also homozygous for the T-DNA insertion site in *AtNHX1*, DNA blots were analyzed for RFLPs about the *AtNHX1* genomic region (Figure 2a). Two bands hybridized to the full-length *AtNHX1* genomic DNA probe in wild-type and negative control lines for the *Bam*HI digest; three distinct bands hybridized in the homozygous line. The heterozygous line appeared to have only four bands as the largest band in wild-type and *nhx1* homozygotes overlapped.

Figure 1. Organization of *AtNHX1* gene.
The genomic region of *AtNHX1* is shown as a line. Exons are shown to scale as boxes, with the 5′ and 3′ UTR of the cDNA shown as light-shaded boxes. The position of the T-DNA insertion is indicated by the triangle. Small arrows indicate the positions of the N-terminal and C-terminal gene-specific primers and the left border primer used to screen the knockout DNA pools.

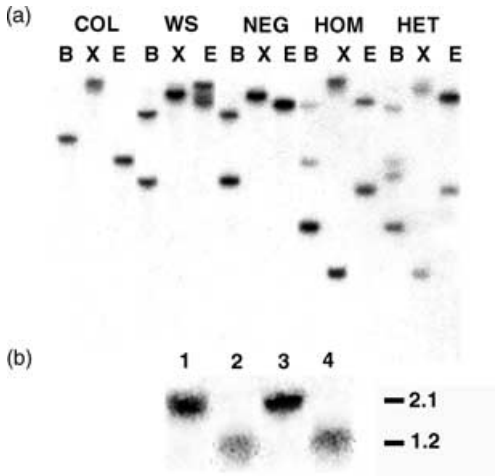

Figure 2. Analysis of T-DNA insertion in *AtNHX1*.
(a) Southern blot of DNA isolated from Columbia wild-type (COL), Wassilewskija wild-type (WS), plants from final pool of seeds not showing T-DNA insertion by PCR (NEG), and plants either homozygous (HOM) or heterozygous (HET) for the T-DNA insertion as determined by PCR and segregation of kanamycin resistance. Genomic DNA was digested with *Bam*HI (B), *Xho*I (X), or *Eco*RI (E), and probed with the 3.4-kb PCR product amplified from wild-type plants using the N-terminal knockout (NKO) and C-terminal knockout (CKO) primers (as shown in Figure 1).
(b) RNA gel blot analysis of 30 μg of RNA isolated from WS wild-type plants (lanes 1 and 3) and homozygous *nhx1* plants (lanes 2 and 4) grown in media containing 1 mM K^+ with the addition of either 0 mM NaCl (lanes 1 and 2) or 100 mM NaCl (lanes 3 and 4). The RNA blot was probed with the full-length cDNA of *AtNHX1*.

To assess the effect of the T-DNA insertion on *AtNHX1* mRNA expression, RNA blot analysis was performed on total RNA isolated from seedlings of wild-type and homozygous *AtNHX1* mutant (*nhx1*) lines grown on 1 mM K^+ with or without the addition of 100 mM NaCl. In both wild-type and mutant lines, *AtNHX1* RNA was slightly more abundant in salt-treated seedlings (lanes 3 and 4 of Figure 2b), but the size of the transcript in the *nhx1* (approximately 1.2 kb) was substantially smaller than that of the full-length mRNA transcript (2.1 kb). These results were consistent with the position of the T-DNA insertion.

AtNHX1 *expression in wild-type* Arabidopsis

Our interest in determining the tissue localization of *AtNHX1* expression was to try to anticipate possible phenotypes of *AtNHX1* mutants. To this end, *in situ* hybridizations with *AtNHX1*-specific RNA probes were performed (Figure 3). Hybridization signals were detected in almost all tissues for antisense, but not sense, RNA probes complementary to a 384-bp region of the 5′-untranslated region

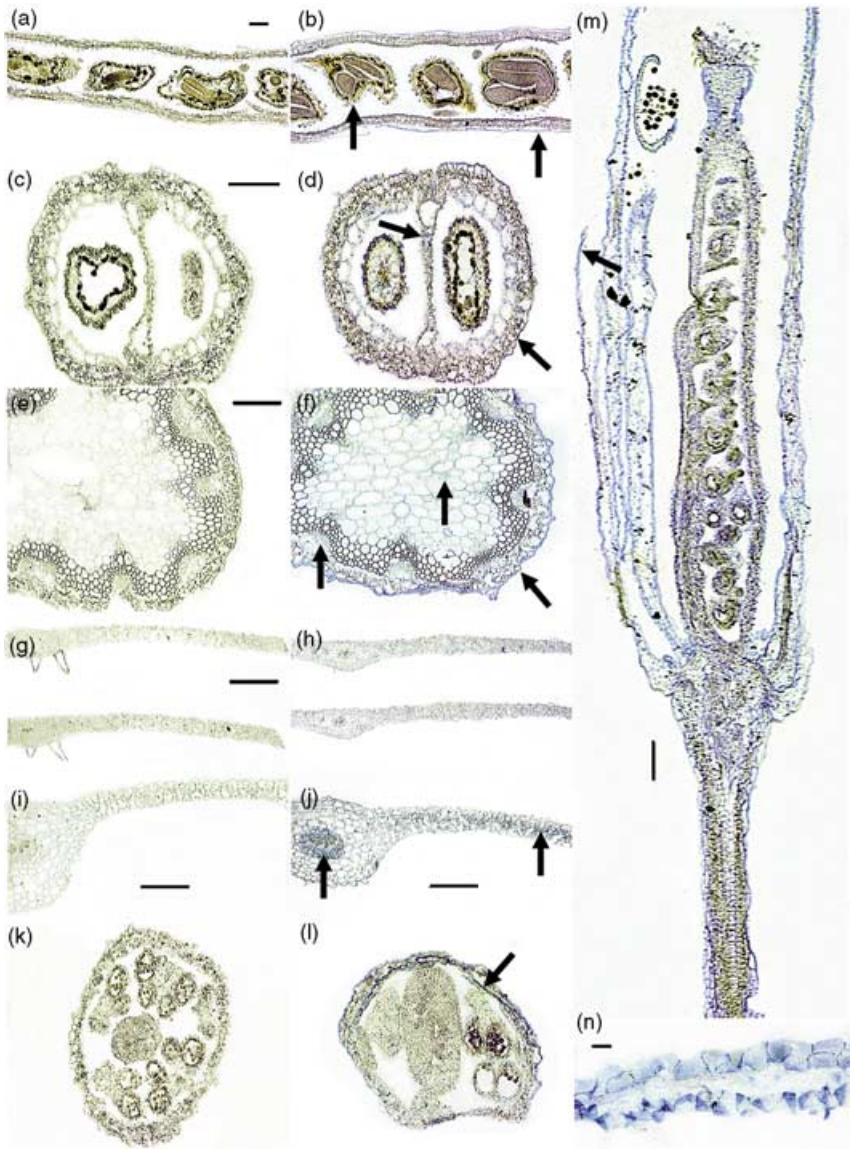

Figure 3. Localization of *nhx1* mRNA in *Arabidopsis* wild-type tissues.
Tissues were fixed, embedded in paraffin, cut into 7-μm-thick sections, and hybridized with a sense (a, c, e, g, i, and k) or antisense (b, d, f, h, j, l, m, and n) RNA probe complementary to a portion of the 5′ UTR of *AtNHX1* as outlined in the section under Experimental procedures. Mature green siliques are shown in (a, b) longitudinal and (c, d) cross-sections.
(e, f) Inflorescence stem cross-section from 4-week-old plants.
(g, h) Cross-sections of younger and (i, j) older leaves.
(k, l) Cross-sections of buds.
(m) Longitudinal section through mature flower and (n) petal. Arrows indicate (b) integument and epidermis, (d) silique septum and epidermis, (f) phloem, cortex and epidermis, (j) phloem and mesophyll, (l) petal, and (m) sepal. All bars = 100 μm except in (n), where bar = 10 μm.

(UTR) of *AtNHX1* cDNA. These signals were strong in certain cell types, in particular, the epidermal layers in siliques, inflorescence stems, leaves, and flowers, especially in petals. Cells around the phloem tissues (see Figure 3f,j) also displayed a strong signal. In siliques, *AtNHX1* signal was seen very strongly in the outer integument. Longitudinal sections of siliques also showed *AtNHX1* signal in the developing embryo. Stem sections also showed *AtNHX1* antisense signal in cortical tissues. In leaves, the intensity of the signal was highest around the vascular tissue, with relatively lower intensity in epidermal and parenchyma tissue. Both young and mature leaves showed the same pattern of signal intensity. Very strong signal intensity was observed in petals, stamens, and anthers. Developing ovaries in floral longitudinal sections showed very little *AtNHX1* hybridization signal.

Effects of NaCl on growth of nhx1 *plants*

As overexpression of AtNHX1 conferred increased tolerance to salinity (Apse *et al.*, 1999), we hypothesized that the absence of AtNHX1 might have the opposite effect, that is, an increased sensitivity to NaCl. We first tested the effect of NaCl on the establishment of seedlings on agar media. In these experiments, we used a slightly modified version of the growth medium described by Spalding *et al.* (1999). We chose this formulation over the traditional Murashige and Skoog medium because it allows for the control of potassium and sodium concentrations, as well as the maintenance of the nitrogen source at a more physiological concentration. Successful seedling establishment was scored as greening of cotyledons, emergence, and expansion of true leaves after 3 weeks on the growth medium. As

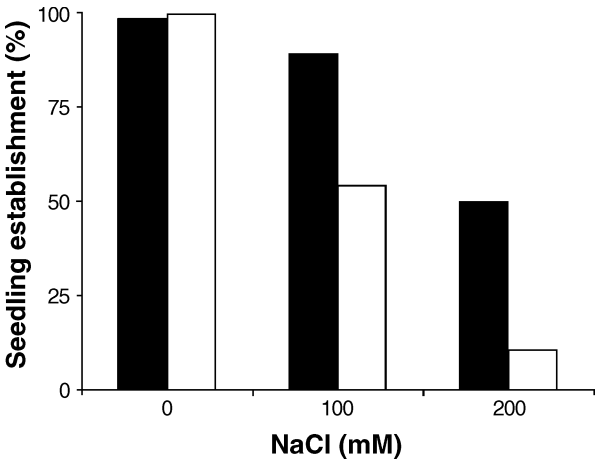

Figure 4. Seedling establishment of wild-type and *nhx1* genotypes. Percentage of wild-type (black bars) and *nhx1* (white bars) seedlings that developed green cotyledons and fully expanded and green true leaves 2 weeks after sowing of seeds on agar media containing 1 mM K^+ that was supplemented with different amounts of NaCl. The response of seedling establishment with NaCl was highly significant ($P < 0.001$ by ANOVA, $n = 250$ for each sample in three independent replicates).

shown in Figure 4, NaCl had a much stronger inhibitory effect on *nhx1* seedlings than it has on the wild type. Only 50% of *nhx1* seedlings were able to grow after 2 weeks at 100 mM NaCl, where wild-type seedlings were inhibited to this level only at 200 mM NaCl. We also used the root-bending assay (Zhu *et al.*, 1998) to test whether root growth in *nhx1* seedlings displayed phenotypical differences. No significant differences in root growth between wild-type and *nhx1* plants were observed when the seedlings were grown for a week in the absence or presence of 100 mM NaCl (results not shown).

For assessment of NaCl effects on mature plants, seedlings were first grown for 2 weeks on media without NaCl and were then transferred to soil. After acclimation, plants were watered with nutrient media with or without 100 mM NaCl. This NaCl concentration was chosen because it was sublethal for wild-type plants (Apse *et al.*, 1999), and we anticipated an increased sensitivity in the mutant line. Plants shown in Figure 5 had been treated for 10 days. We also noted during this set of experiments that the knockout line had a slightly reduced time to bolting and flowering. The most profound visible phenotype in both the control- and salt-treated *nhx1* plants was a marked reduction in leaf area compared to the wild type (Figure 5c versus 5a, 5d versus 5b).

Leaf area and epidermal cell size differences in nhx1

Differences in leaf area between the wild type, *nhx1,* and the *NHX1*-complemented mutant (*NHX1::nhx1*) plants were quantified by measuring the leaf areas of 4-week-old plants grown on soil watered with 1 mM K^+ (Figure 6a). Leaves of *nhx1* plants were between 50 and 65% the area of wild-type and *NHX1::nhx1* leaves at equivalent positions (Figure 6b) except for the young leaves. It appeared that the rate of leaf expansion in the *nhx1* line reached a plateau much earlier than it did in wild-type plants. The wild-type phenotype was recovered by expression of *AtNHX1* cDNA in the *nhx1* background. For leaves 10 and 9, the recovery to wild-type phenotype did not appear to be complete, although the differences at this stage of growth were not that significant. To further investigate this difference in leaf area, leaf abaxial epidermal impressions were quantified for cell area. The images in Figure 7(a–c) are representative images for the basal area of the most fully expanded leaf (leaf 8). There was a wide variation in epidermal cell area for all lines, and the distribution of cell areas was dramatically different. For example, in wild-type leaves, 10–20% of the cells were very large (between 3000 and 6000 μm^2). The frequency of these large epidermal cells was relatively low in the *nhx1* line (see Figure 7d,e). The distribution of epidermal leaf cell areas in the *NHX1::nhx1* line was similar to that in the wild type (Figure 7f).

Cation-dependent H^+ transport in vacuoles isolated from wild-type and nhx1 *plants*

The *nhx1* mutant line makes it possible to assess the contribution of this vacuolar Na^+/H^+ antiporter to ion transport by comparing transport in vacuoles isolated from wild-type and mutant plants. This was assayed by the measurement of rates of cation-dependent H^+ efflux using fluorescence quenching. In plants overexpressing AtNHX1, both Na^+- and K^+-dependent H^+ efflux have been observed (Apse *et al.*, 1999; Zhang and Blumwald, 2001). We hypothesized that a reduction in AtNHX1 antiporters in the mutant line relative to the wild type would cause a reduction in the cation-dependent H^+ efflux, which would be observed as a decrease in the rate of quench recovery (which is proportional to the rate of H^+ efflux; Bennett and Spanswick, 1983). The results are shown in Figure 8. For all types of vacuoles (wild type, *nhx1* mutant, and *NHX1::nhx1*), approximately 60% fluorescence quench was obtained in a period of 25 min following the addition of Mg^{2+} to the assay. In wild-type vacuoles, the rates of quench recovery were higher for Na^+ than for K^+ at 10, 25, and 50 mM cations (Figure 8d). These rates increased with higher concentrations of cations in the assay. The ratio of Na^+- to K^+-dependent quench recovery ranged from 3 : 1 at 10 mM cations to 1.8 : 1 at 50 mM cations in vacuoles isolated from both wild-type and *NHX1::nhx1* plants. In vacuoles isolated from the *nhx1* line, there was only a marginal increase in the quench recovery rate for both Na^+ and K^+ over the range of concentrations assayed. For both K^+ and Na^+, *nhx1* vacuoles displayed approximately 50% higher cation-dependent H^+ efflux in the

Figure 5. Effects of sodium on young seedlings of WS and *nhx1* genotypes.
Wild-type (a, b) and *nhx1* (c, d) plants watered with control (a, c) or 100 mM NaCl (b, d) supplemented solution. Plants are shown at 4 weeks after germination (10 days after start of salinity treatment).

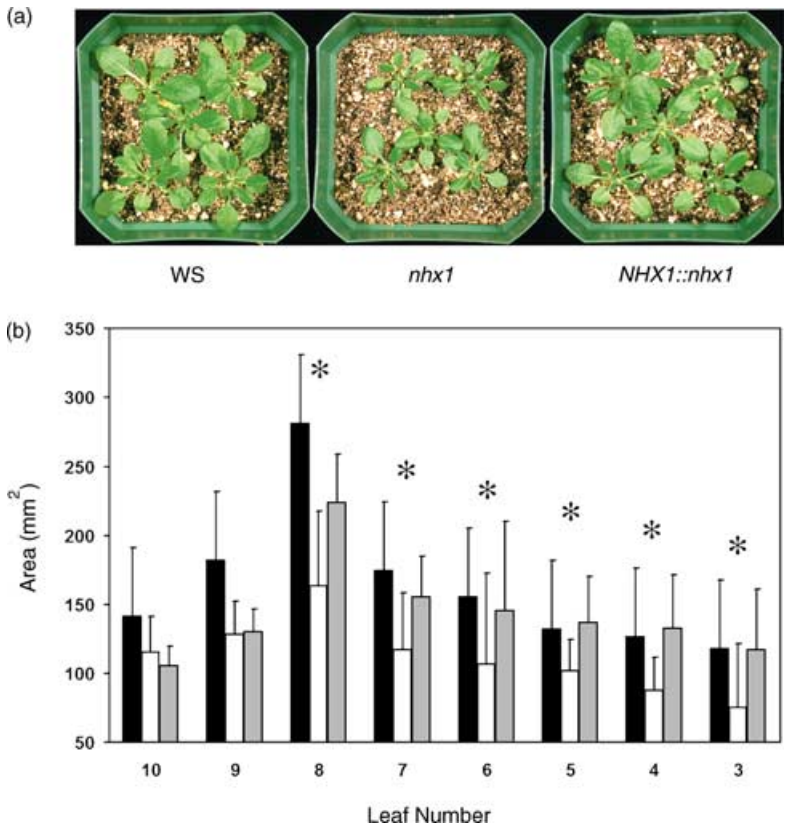

Figure 6. Leaf areas of wild-type, *nhx1*, and *NHX1::nhx1* plants.
(a) Wild-type, *nhx1*, and *NHX1::nhx1* plants grown in soil for 3 weeks following transplantation from agar plates. Plants were watered with a nutrient solution containing 1 mM K^+ as described in the section under Experimental procedures.
(b) Leaf areas of 4-week-old wild-type (black bars), *nhx1* (white bars), and *NHX1::nhx1* (gray bars) plants were measured by image analysis of photocopied leaves. Values are the mean ± SD ($n = 10$–12). Asterisks indicate where wild-type and complemented *nhx1* plants show statistically significant differences ($P < 0.01$) from *nhx1* plants as measured by the Student's *t*-test.

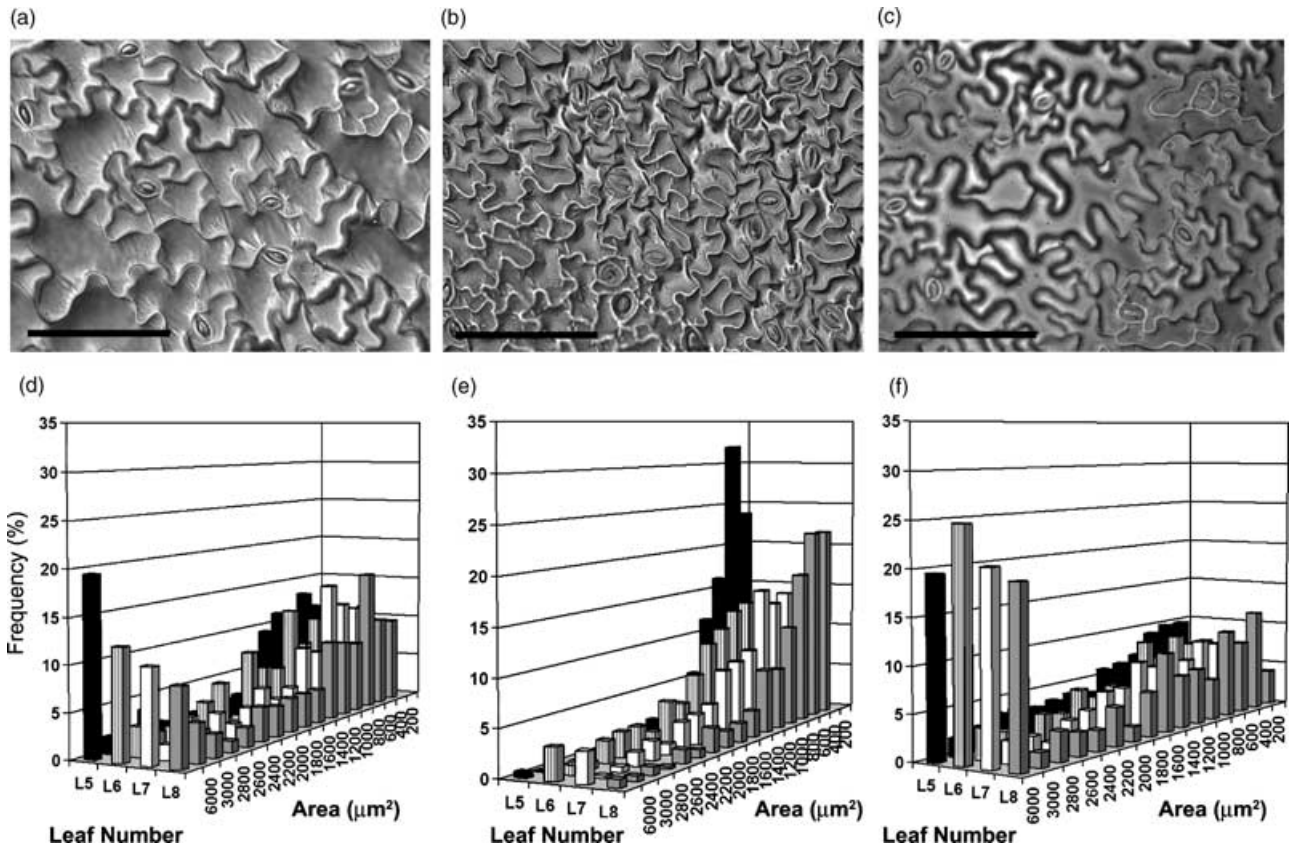

Figure 7. Frequency distribution of leaf epidermal cell size in wild-type and *nhx1* plants.
Bright-field images of epidermal impressions from the basal region of Leaf 8 of (a) wild-type plants, (b) *nhx1* plants, and (c) *NHX1::nhx1* plants; bars = 100 μm. Distributions of epidermal cell areas by leaf number in (d) wild-type plants, (e) *nhx1* plants, and (f) *NHX1::nhx1* plants. Epidermal cell area values greater than 3000 μm^2 were binned into the last category (6000).

presence of 50 mM K^+ or 50 mM Na^+, although these differences were not statistically significant.

Discussion

Of the 17 plant vacuolar Na^+/H^+ antiporter genes that have been cloned thus far, and of the 40 ESTs that show strong similarity to AtNHX1, most belong to salt-sensitive species (Aharon *et al.*, 2003). However, the activity of tonoplast Na^+/H^+ antiporters has been measured primarily in salt-tolerant species. Mennen *et al.* (1990) concluded that Na^+/H^+ antiporters were not an ubiquitous characteristic of all plant cells, based on the lack of pH-dependent $^{22}Na^+$ uptake in excised roots. It is plain to see that, despite the difficulty in measuring vacuolar Na^+/H^+ antiporter activity in salt-sensitive plants, not only are they present in these genomes but also some members are widely and relatively abundantly expressed. All plants must deal with sodium and cytosolic Na^+ toxicity. In the absence of Na^+/H^+ antiporters that could reduce cytosolic Na^+ concentrations, how will plants cope with the inevitable influx of Na^+? Mechanisms that reduce sodium uptake might include K^+ channels and/or transporters that have a higher K^+ to Na^+ selectivity ratio. Another alternative is sodium efflux via an Na^+-ATPase. Although an Na^+-transporting ATPase has been cloned from the unicellular chrysophyte *Heterosigma akashiwo* (Shono *et al.*, 2001), homologous sequences and similar transport activities have not been detected in higher plants. The other consideration is that these sodium proton exchanger (NHX) proteins fulfill multiple roles in the plant kingdom.

Here, we have shown that one of the vacuolar Na^+/H^+ antiporters in *Arabidopsis*, AtNHX1, is expressed in many different tissues of the plant. This can imply that either there are many different roles filled by AtNHX1 or the same role is filled in many different tissues (or both). Yamaguchi *et al.* (2001) showed that in flower petals, the AtNHX1 homolog in morning glory (*Ipomoea nil*) mediates a developmentally regulated vacuolar alkalinization in the transition of purple buds to blue flowers. This alkalinization changes the absorption spectrum of the anthocyanins stored in the vacuole. AtNHX1 is strongly expressed in floral tissues, not only in petals but in stamens and anthers as well. *AtNHX1* mRNA was not detected early in ovule development but

was quite strongly expressed in the outer integument in maturing siliques. This expression pattern argues for roles for AtNHX1 in flower, pollen, and seed development that are not related to floral coloration (at least in *Arabidopsis*). We also observed that AtNHX1 transcripts in inflorescence stems and in leaves in cells closely associated with the vascular tissue. Given the biochemical function of AtNHX1 (i.e. cation/H^+ exchange), we can hypothesize that expression in these tissues may be important in maintaining a balanced ion distribution, whether this be a balance of Na^+, K^+, or both. Cells adjacent to the xylem stream will act as a source of ions for distribution to neighboring cells. It is interesting that the induction of AtNHX1, as determined by promoter-GUS fusion analysis, in response to salinity treatment of seedlings is very strong, especially in the root vascular tissues (Shi and Zhu, 2002).

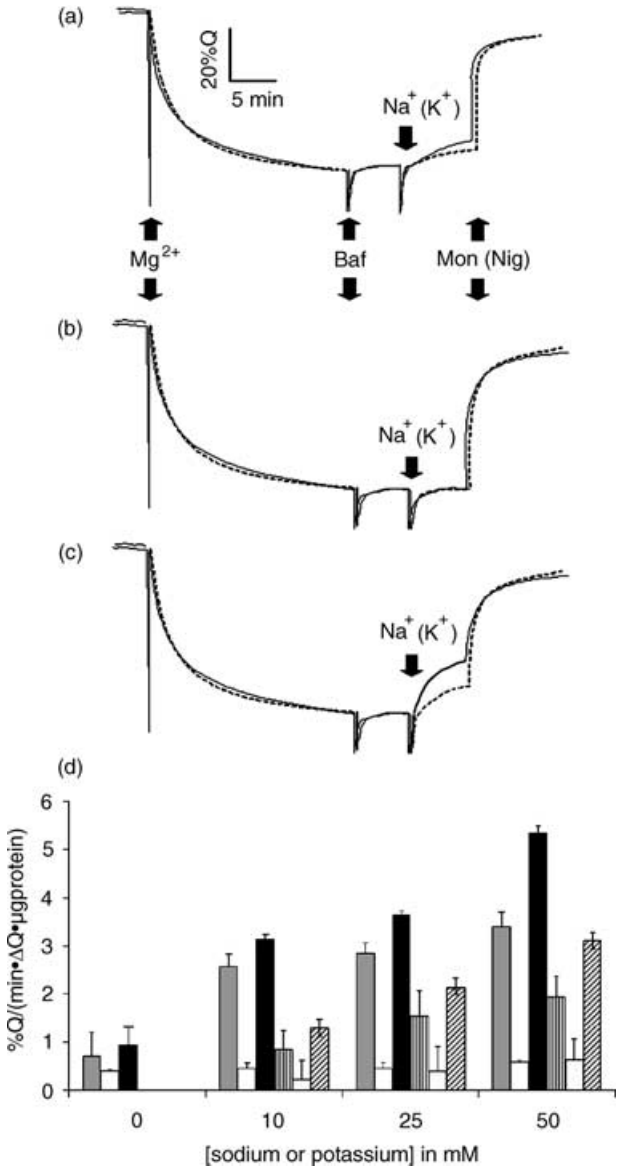

It has been shown previously that AtNHX1 conferred salinity tolerance to plants that overexpressed the gene (Apse *et al.*, 1999; Zhang and Blumwald, 2001; Zhang *et al.*, 2001). Now, the identification of a T-DNA insertional mutant of AtNHX1 has made it possible to assess the contribution of AtNHX1 to ion homeostasis in wild-type plants. There are two phenotypes of the *nhx1* plants that are directly related to the movement of sodium across the tonoplast membrane. The first is the tolerance of the germinating seed and seedling to sodium. Wild-type seeds were able to establish viable seedlings at higher concentrations of NaCl than were the *nhx1* seeds. The loss of AtNHX1 did not affect seedling establishment in the absence of NaCl. It is possible that the expression of AtNHX1 in the embryo (as seen in the longitudinal sections of mature siliques) is an important factor for NaCl tolerance at germination. An additional factor in the reduced vigor of *nhx1* seeds might be the supply of nutrients to the developing embryo in the maturing silique – AtNHX1 may contribute to the transport of K^+ (and/or Na^+) reaching the developing embryo. It has been demonstrated that more than 90% of the water transported into the expanding fruit of tomato occurs through the phloem (Davies *et al.*, 2000). Thus, the ability to maintain a high cytosolic K^+/Na^+ concentration ratio along the symplastic pathway may be important for seedling vigor. Leaf area was reduced in the *nhx1* plants. This leaf area difference was evident in young leaves and persisted to fully expanded leaves. Much of the difference in leaf area is correlated to the reduction in frequency of the very large epidermal cells. Our hypothesis for this phenomenon is that the lack of AtNHX1, which mediates K^+ and pH homeostasis in cells, has an impact on the ability of these cells to expand. It is the large central vacuole that effectively reduces the surface to volume ratio in plant cells and provides the turgor necessary for cell expansion.

Figure 8. Cation-dependent H^+ transport in vacuoles isolated from wild-type and *nhx1* plants.

Proton movements were monitored by following the fluorescence quenching of acridine orange as described in the section under Experimental procedures. At the indicated times (Mg^{2+}), vacuolar acidification was initiated by the addition of 3 mM $MgSO_4$. After a steady-state acidic-inside pH gradient was attained, the activity of the H^+-ATPase was stopped by the addition of 10 nM bafilomycin (Baf). After a steady-state leak was attained, Na^+ or K^+ was added as NaCl or KCl. The pH gradient was collapsed by the addition of monensin (Mon-artificial Na^+/H^+ antiporter) or nigericin (Nig-artificial K^+/H^+ antiporter).

(a) Vacuoles isolated from wild-type plants, 25 mM Na^+ (solid line) or K^+ (dashed line).

(b) Vacuoles from *nhx1* plants, 25 mM Na^+ (solid line) or K^+ (dashed line).

(c) Vacuoles from *NHX1::nhx1* plants, 25 mM Na^+ (solid line) or K^+ (dashed line). Traces are representative of six independent experiments.

(d) Rates of Na^+-dependent H^+ efflux in vacuoles isolated from wild-type (gray bars), *nhx1* (white bars), and *NHX1::nhx1* plants (black bars). Rates of K^+-dependent H^+ efflux in vacuoles isolated from wild-type (vertical bars), *nhx1* (dotted bars), and *NHX1::nhx1* plants (diagonal bars). These initial rates were taken within the first 2 min after the addition of NaCl or KCl. The rates were normalized both to the fluorescence change between the addition of Mg^{2+} and the addition of bafilomycin (ΔQ) and to the amount of protein present in each assay. Values are mean ± SD ($n = 4$).

The yeast NHX1 homolog has been implicated in vacuolar biogenesis (Nass and Rao, 1998) and shown to be important for protein trafficking out of the pre-vacuolar compartment (Bowers *et al*., 2000). In both cases, it is the Na^+/H^+ exchange activity that is thought to be important for this function. If AtNHX1 has an analogous function in plant cells, the regulation of protein sorting or the development of the central vacuole could be perturbed so as not to permit the expansion of the epidermal cells beyond a threshold. We cannot exclude the possibility that the phenotypes we observed could be because of an effect on sorting at the plant vacuole; nonetheless, the activity of the H^+-ATPase in vacuoles from both wild-type and *nhx1* plants was similar.

The distribution of epidermal cell size in the *nhx1* plants shows that it is primarily the very large cells that are reduced in frequency. These large epidermal cells in wild-type leaves have been shown to have polyploid nuclei (Kondorosi *et al*., 2000). For cells with polyploid nuclei, DNA replication takes place without mitosis. It has been suggested that this endoreduplication takes place before cell expansion (Kondorosi *et al*., 2000). Whether the lack of AtNHX1 inhibited the endoreduplication process or the expansion process in the *nhx1* plants remains to be investigated. Ion homeostasis may have a close connection with cell cycle regulation. Yenush *et al*. (2002) have recently shown that there is a relationship between the K^+ and pH status of yeast cells and cell cycle regulation. The loss of AtNHX1 in the knockout plants may cause an altered K^+ and pH balance in the cells, which may affect similar cell cycle regulation processes in plants. The lack of a phenotypical difference between wild-type and *nhx1* plants as measured with the root-bending assay can be explained by the action of other mechanisms for H^+/cation exchange (both at a tissue and cellular level). AtNHX4 is a vacuolar AtNHX isoform that is expressed primarily in roots (Aharon *et al*., 2003; AtNHX4 *sensu* Mäser *et al*., 2001 is equivalent to AtNHX3 described by Yokoi *et al*., 2002). This form may suffice for normal vacuolar cation accumulation in roots, thus compensating for the lack of AtNHX1. The measurement of both K^+/H^+ and Na^+/H^+ exchange definitively points to AtNHX1 as the dominant cation/H^+ antiporter on the vacuolar membrane in leaf tissues. The differences in Na^+- and K^+-dependent H^+ transport in wild-type and *nhx1* vacuoles strongly support the exchange activities attributed to AtNHX1 overexpression in tomato (Zhang and Blumwald, 2001). Under conditions of potassium deficiency, cytosolic K^+ is maintained by mobilization of vacuolar K^+ cytosolic K^+ concentrations begin to decline only when the vacuolar K^+ concentration reaches concentrations below 20 mM (Leigh and Jones, 1984). The distribution of cytosolic and vacuolar potassium is likely to be mediated, in part at least, by AtNHX1. Although there was a residual H^+ efflux in the *nhx1* vacuoles after the inhibition of the vacuolar H^+-ATPase, this was small relative to that present in wild-type vacuoles. This residual activity may be because of the presence of other vacuolar Na^+/H^+ antiporters. The cation proton antiporter 1 (CPA1) family of *Arabidopsis* cation/H^+ antiporters includes eight members named AtNHX (Mäser *et al*., 2001; Ward, 2001). AtNHX7 has been identified as AtSOS1 and shown to be a plasma membrane Na^+/H^+ antiporter (Shi *et al*., 2000). AtNHX8 is highly similar to AtNHX7 (AtSOS1) and is also most probably a plasma membrane transporter. AtNHX1–6 have a significant similarity to the endosomal NHX from yeast (Aharon *et al*., 2003; Yokoi *et al*., 2002). According to their amino acid sequence similarity, the vacuolar AtNHX antiporters can be grouped into two different subgroups, AtNHX1–4 and AtNHX5–6. While the first group is >75% similar, the second group is <40% similar to the first. Despite this primary sequence difference, AtNHX1–5 have functional Na^+/H^+ antiporter activity based on their ability to complement the endosomal yeast NHX (Aharon *et al*., 2003; Yokoi *et al*., 2002). Immunological and green fluorescent protein (GFP) expression studies have shown that AtNHX1 (Apse *et al*., 1999), AtNHX2 (Yokoi *et al*. 2002), and AtNHX5 (Duan, 2001) are localized to the vacuole. Of the six AtNHX1-like genes in *Arabidopsis*, two are expressed in leaves (Aharon *et al*., 2003) and may account for this residual activity.

The data presented here support the role of AtNHX1 in the maintenance of K^+ (and Na^+) homeostasis in plants. In the *nhx1* plants, the lack of AtNHX1 activity affects seedling establishment and the development of leaf epidermal cells.

It has recently been shown that transgenic *Brassica napus* plants overexpressing AtNHX1 did not display an enhanced production of cysteine or glutathione in response to salt stress (Ruiz and Blumwald, 2002). These results suggested that ion homeostasis and vacuolar Na^+ accumulation (with the concomitant high cytosolic K^+/Na^+ ratio) are important components in the response of the transgenic plants to salt stress. The *nhx1 Arabidopsis* plants provide a unique tool complementary to studies with ectopic overexpression of AtNHX1 to further investigate the role of ion homeostasis in processes such as stress tolerance and development.

Experimental procedures

T-DNA-tagged nhx1 *mutant isolation*

DNA pools of *Arabidopsis* T-DNA insertion lines from the ALPHA population collection at the *Arabidopsis* Knockout Facility (University of Wisconsin (http://www.biotech.wisc.edu/Arabidopsis/) were screened for T-DNA insertion in the *AtNHX1* locus. Forward and reverse primers from the coding sequence of the *AtNHX1* locus were designed for PCR screening of the DNA pools in combination with the T-DNA left-border-specific primer. The primers were designed using the cDNA sequence of AtNHX1 from the Columbia ecotype as genomic sequence for AtNHX1 was not available. These primers are as follows: JL-202 (left border primer),

5′-CATTTTATAATAACGCTGCGGACATCTAC-3′; X1XNTKO (located 183 nucleotides upstream of the start codon), 5′-CTTGTATTGT-TCTTGGTCATCTTTTGGAA-3′; X1XCTKO (located 97 nucleotides upstream of the stop codon), 5′- TCATCAAATTGTCTCCAGTAG-TAATGCAC-3′. PCR products were analyzed by DNA gel blot hybridization to the AtNHX1 gene probe generated from amplification of genomic DNA with the N-terminus- and C-terminus-specific primers. A positive PCR product, approximately 1-kb long was identified from Superpool-27 for reactions with XIXCTKO and JL-202. Sequencing of this product and the one amplified from the secondary pool CSH240 confirmed that the insertion was within the coding region of AtNHX1. Homozygous mutant plants, grown from the final pool #CSJ5984, determined as homozygous for kanamycin-resistant growth on agar media were confirmed by Southern blot analysis using the AtNHX1 gene probe and PCR with primers internal to X1XCTKO and X1XNTKO.

Complementation of nhx1 *mutant line*

Homozygous *nhx1* plants were transformed by *Agrobacterium* (GV3101) using the floral dipping method. The transforming vector was constructed by ligation of a PCR-amplified *AtNHX1* open-reading frame into a pCAMBIA1200 vector. In this construct, AtNHX1 expression is driven by the CAMV35S promoter. The selectable marker is hygromycin resistance, as the T-DNA knock-out line already contains NPTII (KanR). Selection of transformants was on 0.5× MS agar medium supplemented with 25 mg l^{-1} hygromycin and 500 mg l^{-1} vancomycin. Single-copy lines homozygous for the complementing T-DNA were isolated by segregation analysis on selection media of T_2 and T_3 lines. The lines selected for complementation phenotyping experiments were homozygous for a single insertion event. T_3 seeds were used in all experiments. Northern analyses confirmed that the expression levels of *AtNHX1* in the *NHX1::nhx1* lines were increased by about 50% as compared to the expression levels in wild-type plants as determined by both phosphoimaging and DNA microarray experiments (data not shown).

Plant material and growth treatments

Seeds of *Arabidopsis thaliana* ecotype Wassilewskija (WS) or of the homozygous T-DNA insertional mutant (WS background) were sterilized in 15% commercial bleach, 0.0025% SDS for 15 min, followed by extensive washes with sterile water. Seeds were imbibed at 4°C for 3–4 days in the dark and then sown on media as described below. The growth medium is a modification of that described by Spalding *et al.* (1999) and contained 2.5 mM $Ca(NO_3)_2$, 2 mM $MgSO_4$, 80 μM $Ca(H_2PO_4)_2$, 25 μM $CaCl_2$, 25 μM H_3BO_3, 2 μM $MnSO_4$, 0.5 μM Na_2MoO_4, 0.5 μM $CuSO_4$, 0.01 μM $CoCl_2$, 2 μM $ZnSO_4$, 0.1 mM Na_2EDTA, 0.1 mM $FeSO_4$, 100 mg l^{-1} myo-inositol, 0.5 mg l^{-1} nicotinic acid, 0.5 mg l^{-1} pyridoxine-HCl, 0.5 mg l^{-1} thiamine-HCl, 2 mg l^{-1} glycine, 0.7% agar (plant cell culture grade). pH was adjusted to 5.7 with 1N KOH and KCl was adjusted to 1 mM with 1 M KOH. For growth of seedlings prior to transplantation to soil, 0.5% sucrose was added to the medium to speed growth.

The watering treatment (with or without 100 mM NaCl) began 5 days after transplanting 2-week-old agar plate-grown seedlings to soil. Plants were watered every 3 days with enough watering solution (150 ml) to thoroughly wet the soil in the pot and leach 10–20 ml per pot. The duration of the watering treatment was 21 days.

Root growth measurements were performed according to Zhu *et al.* (1998). Briefly, 4-day-old seedlings (germinated as described above in vertical agar plates) were transferred to agar plates containing the growth media described above, with or without 100 mM NaCl. The treatment plates were placed vertically with seedlings in the upright position, and increases in root length were measured with a ruler every day for 7 days (Zhu *et al.*, 1998).

In situ *hybridization*

A unique region of the AtNHX1 cDNA was selected for amplification of probe templates so that we could be certain that signals, when detected, were specific for AtNHX1. The following primer pair, given here as gene name, region of the cDNA from which it was amplified, amplicon size, and then primer pair were used to amplify the PCR product for cloning into the pSPT18 and pSPT19 cloning vectors (Roche, Indianapolis, IN, USA): AtNHX1, 5′ UTR, 348 bp, X1ECO 5′-GAATTCGCCTCTCTGTTTCGTTCCTC-3′, X1PST 5′-CTGCAGACCACAGAAGCGTGATCAGA-3′. Digoxigenin (DIG)-labeled sense and antisense probes were synthesized, and labeling efficiency was evaluated according to manufacturer's instructions (DIG RNA Labeling Kit, Roche, Indianapolis, IN, USA).

In situ hybridization was performed as described by Long *et al.* (1996), except for the following modifications. *Arabidopsis thaliana* ecotype Columbia plant tissues were fixed in 4% paraformaldehyde and dehydrated through an ethanol and ter-butyl alcohol series before embedding in paraffin. Sections of 7 μm thickness were adhered to ProbeOn Plus slides (Fisher, Pittsburgh, PA, USA), deparaffinized with Histoclear, rehydrated through an ethanol series, treated for 30 min with 1 μg ml^{-1} proteinase K, re-fixed with paraformaldehyde, treated with 0.1 M acetic anhydride, and dehydrated through an ethanol series. Slide pairs were incubated with equal concentrations of sense and antisense probes at 55°C overnight. Post-hybridization treatment, including washes and RNAse treatment, was also as described by Long *et al.* (1996). Alkaline-phosphatase-conjugated anti-DIG antibodies were used to detect DIG-labeled probes. Nitroblue tetrazolium (NBT)/5-bromo-4-chloro-3-indolyl phosphate (BCIP) (Invitrogen, Carlsbad, CA, USA) was incubated with the slides to generate a color reaction with the alkaline phosphatase bound to the antibody. Slides were dehydrated and mounted with Permount (Sigma, St Louis, MO, USA).

Leaf area and epidermal cell measurements

Areas were determined for leaves of 4-week-old *A. thaliana* (ecotype WS), homozygous *nhx1*, or *NHX1::nhx1* plants grown on soil supplemented with 1 mM K^+ as described above. Leaves 12 through 3 were cut and immediately photocopied at high contrast to provide images suitable for analysis with SCION IMAGE software (http://www.scioncorp.com). Negative impressions of abaxial epidermal cells from leaves of plants grown as described above were made with ProvilNovo LightCD dental impression medium (Heraeus, Germany). A positive impression was obtained by painting nail polish to the negative impression. This layer of polish was then viewed under bright-field illumination. Images viewed on a Nikon E600 microscope were captured using a SPOT digital camera and software (Diagnostic Instruments, Sterling Heights, MI, USA). Epidermal cell areas were determined using SCION IMAGE software.

Vacuolar transport assays

Vacuoles were isolated from leaves of 3-week-old *A. thaliana* (ecotype WS) or homozygous *nhx1* seedlings grown on agarose medium supplemented with 1 mM K^+ as described above.

Vacuoles were isolated as described previously by Apse *et al.* (1999). The fluorescence quenching of acridine orange was used to monitor the establishment and dissipation of inside-acidic pH gradients between the vacuolar lumen and the assay buffer. Vacuoles (200 μl, containing approximately 1.8 μg total protein) were added to give a final 0.8 ml volume of buffer containing 0.3 M mannitol, 2 mM dithiothreitol, 2.5 mM Tris-MES buffer (pH 8.0), 1.5 mM Tris-ATP, 5 μM acridine orange, and 50 mM Cl^- supplied as a combination of tetramethylammonium-Cl (TMA-Cl) and either NaCl or KCl. Vacuolar acidification was initiated with the addition of 3 mM Mg^{2+}, and the change of fluorescence with time was monitored on PerkinElmer Fluorescence Spectrophotometer with excitation wavelength of 495 nm and slit width of 2.5 nm and emission wavelength of 540 nm and 10 nm slit width with a 1% transmittance filter between the cuvette and the photomultiplier tube. When a steady-state pH gradient (acidic inside) was formed, bafilomycin was added to a final concentration of 10 nM to inhibit the vacuolar H^+-ATPase. Monensin or nigericin was added to abolish the pH gradient and recover the quenched fluorescence. Quantification of initial rates of acidification and fluorescence recovery was done with FLWINLAB software package (PerkinElmer, Wellesley, MA, USA). Traces were normalized by setting the arbitrary fluorescence scale to 100. Rates of fluorescence recovery after the inhibition of the H^+-ATPase were normalized to the fluorescence quench attained in the assay just prior to the addition of bafilomycin.

Acknowledgements

The authors wish to thank the labs of Nancy Dengler and Neelima Sinha for their assistance with *in situ* hybridizations and epidermal cell area measurements. We also thank Huazhong Shi for technical assistance and critical assessment of the manuscript. This research was supported by a grant from the National Science Foundation (IBN-0110622).

References

Aharon, G.S., Apse, M.P., Duan, S., Hua, X. and Blumwald, E. (2003) Characterization of a family of vacuolar Na^+/H^+ antiporters in *Arabidopsis thaliana*. *Plant Soil*, **253**, 245–256.

Apse, M.P., Aharon, G.S., Snedden, W.A. and Blumwald, E. (1999) Salt tolerance conferred by overexpression of a vacuolar Na^+/H^+ antiport in *Arabidopsis*. *Science*, **285**, 1256–1258.

Barkla, B.J., Zingarelli, L., Blumwald, E. and Smith, J.A.C. (1995) Tonoplast Na^+/H^+ antiport activity and its energization by the vacuolar H^+-ATPase in the halophytic plant *Mesembryanthermum crystallinum* L. *Plant Physiol.* **109**, 549–556.

Bennett, A.B. and Spanswick, R.M. (1983) Optical measurements of ΔpH and ΔΨ in corn root membrane vesicles: kinetic analysis of Cl^- effects on a proton-translocating ATPase. *J. Membr. Biol.* **71**, 95–107.

Blumwald, E. and Poole, R.J. (1985) Na^+/H^+ antiport in isolated tonoplast vesicles from storage tissue of *Beta vulgaris*. *Plant Physiol.* **78**, 163–167.

Blumwald, E., Aharon, G.S. and Apse, M.P. (2000) Sodium transport in plant cells. *Biochim. Biophys. Acta*, **1465**, 140–151.

Bowers, K., Levi, B.P., Patel, F.I. and Stevens, T.H. (2000) The sodium/proton exchanger Nhx1p is required for endosomal protein trafficking in the yeast *Saccharomyces cerevisiae*. *Mol. Biol. Cell*, **11**, 4277–4294.

Chauhan, S., Forsthoefel, N., Ran, Y.Q., Quigley, F., Nelson, D.E. and Bohnert, H.J. (2000) Na^+/myo-inositol symporters and Na^+/H^+-antiport in *Mesembryanthemum crystallinum*. *Plant J.* **24**, 511–522.

Darley, C.P., Wuytswinkel, O.C.M., van der Woude, K., Mager, W.H. and de Boer, A.H. (2000) *Arabidopsis thaliana* and *Saccharomyces cerevisiae NHX1* genes encode amiloride sensitive electroneutral Na^+/H^+ exchangers. *Biochem. J.* **351**, 241–249.

Davies, W.J., Bacon, M.A., Thompson, D.S., Sobeih, W. and Rodriguez, L.G. (2000) Regulation of leaf and fruit growth in plants growing in drying soil: exploitation of the plants' chemical signaling system and hydraulic architecture to increase the efficiency of water use in agriculture. *J. Exp. Bot.* **51**, 1617–1626.

Duan, S. (2001) *Molecular Characterization of AtNHX5, a Vacuolar Sodium/Proton Antiporter*. MSc Thesis, University of Toronto.

Gaxiola, R.A., Rao, R., Sherman, A., Grisafi, P., Alper, S.L. and Fink, G.R. (1999) The *Arabidopsis thaliana* proton transporters, AtNhx1 and Avp1, can function in cation detoxification in yeast. *Proc. Natl. Acad. Sci. USA*, **96**, 1480–1485.

Hamada, A., Shono, M., Xia, T., Ohta, M., Hayashi, Y., Tanaka, A. and Hayakawa, T. (2001) Isolation and characterization of a Na^+/H^+ antiporter gene from the halophyte *Atriplex gmelini*. *Plant Mol. Biol.* **46**, 35–42.

Kondorosi, E., Roudier, F. and Gendreau, E. (2000) Plant cell-size control: growing by ploidy? *Curr. Opin. Plant Biol.* **3**, 488–492.

Leigh, R.A. and Jones, R.G.W. (1984) A hypothesis relating critical potassium concentrations for growth to the distribution and functions of this ion in the plant-cell. *New Phytol.* **97**, 1–13.

Long, J.A., Moan, E.I., Medford, J.I. and Barton, M.K. (1996) A member of the KNOTTED class of homeodomain proteins encoded by the *STM* gene of *Arabidopsis*. *Nature*, **379**, 66–69.

Mäser, P., Thomine, S., Schroeder, J.I. *et al.* (2001) Phylogenetic relationships within cation transporter families of *Arabidopsis*. *Plant Physiol.* **126**, 1646–1667.

Mennen, H., Jacoby, B. and Marschner, H. (1990) Is sodium proton antiport ubiquitous in plant cells? *J. Plant Physiol.* **137**, 180–183.

Nass, R. and Rao, R. (1998) Novel localization of a Na^+/H^+ exchanger in a late endosomal compartment of yeast-implications for vacuole biogenesis. *J. Biol. Chem.* **273**, 21054–21060.

Ruiz, J.M. and Blumwald, E. (2002) Salinty-induced glutathione synthesis in *Brassica napus*. *Planta*, **214**, 965–969.

Shi, H. and Zhu, J.-K. (2002) Regulation of the vacuolar Na^+/H^+ antiporter gene *AtNHX1* expression by salt stress and ABA. *Plant Mol. Biol.* **50**, 543–550.

Shi, H.Z., Ishitani, M., Kim, C.S. and Zhu, J.K. (2000) The *Arabidopsis thaliana* salt tolerance gene SOS1 encodes a putative Na^+/H^+ antiporter. *Proc. Natl. Acad. Sci. USA*, **97**, 6896–6901.

Shono, M., Wada, M., Hara, Y. and Fujii, T. (2001) Molecular cloning of Na^+-ATPase cDNA from a marine alga, *Heterosigma akashiwo*. *Biochim. Biophys. Acta*, **1511**, 193–199.

Spalding, E.P., Hirsch, R.E., Lewis, D.R., Qi, Z., Sussman, M.R. and Lewis, B.D. (1999) Potassium uptake supporting plant growth in the absence of AKT1 channel activity – inhibition by ammonium and stimulation by sodium. *J. Gen. Physiol.* **113**, 909–918.

Venema, K., Quintero, F.J., Pardo, J.M. and Donaire, J.P. (2002) The *Arabidopsis* Na^+/H^+ exchanger AtNHX1 catalyzes low affinity Na^+ and K^+ transport in reconstituted liposomes. *J. Biol. Chem.* **277**, 2413–2418.

Ward, J.M. (2001) Identification of novel families of membrane proteins from the model plant *Arabidopsis thaliana*. *Bioinformatics*, **17**, 560–563.

Xia, T., Apse, M.P., Aharon, G.S. and Blumwald, E. (2002) Identification and characterization of a NaCl-inducible vacuolar Na^+/H^+ antiporter in *Beta vulgaris*. *Physiol. Plant.* **116**, 206–212.

Yamaguchi, T., Fukada-Tanaka, S., Inagaki, Y., Saito, N., Yonekura-Sakakibara, K., Tanaka, Y., Kusumi, T. and Iida, S. (2001)

Genes encoding the vacuolar Na^+/H^+ exchanger and flower coloration. *Plant Cell Physiol.* **42**, 451–461.

Yenush, L., Mulet, J.M., Arino, J. and Serrano, R. (2002) The Ppz protein phosphatases are key regulators of K^+ and pH homeostasis: implications for salt tolerance, cell wall integrity and cell cycle progression. *EMBO J.* **21**, 920–929.

Yokoi, S., Quintero, F.J., Cubero, B., Ruiz, M.T., Bressan, R.A., Hasegawa, P.M. and Pardo, J.M. (2002) Differential expression and function of *Arabidopsis thaliana* NHX Na^+/H^+ antiporters in the salt stress response. *Plant J.* **30**, 529–539.

Zhang, H.-X. and Blumwald, E. (2001) Transgenic salt tolerant tomato plants accumulate salt in foliage but not in fruit. *Nat. Biotechnol.* **19**, 765–768.

Zhang, H.-X., Hodson, J., Williams, J.P. and Blumwald, E. (2001) Engineering salt-tolerant *Brassica* plants: characterization of yield and seed oil quality in transgenic plants with increased vacuolar sodium accumulation. *Proc. Natl. Acad. Sci. USA*, **98**, 12832–12836.

Zhu, J.-K., Liu, J. and Xiong, L. (1998) Genetic analysis of salt tolerance in *Arabidopsis*: evidence for a critical role of potassium nutrition. *Plant Cell*, **10**, 1181–1191.